-

Normal mode oscillations for the circular and dipolar states of a filled hexagonal magnetic dipole cluster

Peter T. Haugen (Corresponding author),[1] Andrew D. P. Smith,[2] and Boyd F. Edwards[1]
[1)]*Department of Physics, Utah State University, Logan, Utah 84322, USA*
[2)]*St. John's College, University of Cambridge, Cambridge CB2 1TP, UK*

(*Electronic mail: phaugen@gmail.com)

We analyze the rotational dynamics of six magnetic dipoles of identical strength at the vertices of a regular hexagon with a variable-strength dipole in the center. The seven dipoles spin freely about fixed axes that are perpendicular to the plane of the hexagon, with their dipole moments directed parallel to the plane. Equilibrium dipole orientations are calculated as a function of the relative strength of the central dipole. Small-amplitude perturbations about these equilibrium states are calculated in the absence of friction and are compared with analytical results in the limit of zero and infinite central dipole strength. Normal modes and frequencies are presented. Bifurcations are seen at two critical values of the central dipole strength, with bistability between these values.

Bifurcations are at the heart of nonlinear dynamics and play a critical role in technology. We present a simple system with a straightforward physical interpretation that nonetheless exhibits bifurcations and bistability. Examining a set of magnets in a "filled hexagon" consisting of a ring of six magnets with a seventh magnet at its center and varying the strength of the central magnet, we predict two different sets of vibrational behavior corresponding to the extreme values of the central dipole. These regimes overlap, leading to bistability.

I. INTRODUCTION

Dipoles are the simplest magnetic objects yet found and the second simplest term in multipole expansions. Collections of dipoles can be used to make magnetomechanical systems used for latches, gears, bearings, and other devices where low friction and high longevity are valued.[1–3]

Bifurcations and catastrophes are important nonlinear phenomena that are integral to the understanding of the buckling of structures under pressure such as bridges and carbon nanotubes.[4]

With this in mind, we consider how simple systems comprised of small numbers of spherical magnets can offer an environment for detailed examination of these phenomena and more. This is in contrast with the higher dimensionality typically associated with systems that exhibit such nonlinear behaviors.

Systems with small numbers of dipoles have been explored previously. Pollack examined the rotation of two dipoles that are free to spin about fixed axes.[5] Stump et al. investigated the normal modes for arbitrary numbers of dipoles that are fixed at the vertices of a regular polygon.[6] Kantorovich et al. find that ring formation is a significant contributor to anomalous behavior in the magnetic response of a ferrofluid at low temperatures.[7] Edwards et al. illustrate the fact that a uniformly magnetized sphere not only generates magnetic fields as though it were a point dipole, but that pairs of such spheres interact with each other as if they were point dipoles.[8] Experiments in the self assembly of a 32-pole cluster validate this equivalence,[9] which simplifies the examination of a sphere that slides freely along the surface of another fixed sphere,[10] the dynamics of a free sphere bouncing against a fixed sphere,[11,12] and isomorphisms between the dynamics of two freely sliding spheres and physical pendulums.[13]

We consider a system of six identical dipoles at the vertices of a regular hexagon and a seventh dipole fixed at the center. The central dipole is identical to the six perimeter dipoles except that

its dipole strength is variable. All seven are constrained to spin frictionlessly on axes so their dipole moments remain coplanar with the hexagon. To find equilibrium states, we begin with the solution of Stump et al. that applies for a central dipole of zero strength.[6] We then construct equilibrium states for finite central dipole strength by increasing the central dipole strength incrementally and introducing an effective drag in Lagrange's equations to enable the system to relax until the net torque on each dipole vanishes. These equilibrium states agree with those obtained by Smith et al. by minimizing the magnetostatic potential energy.[14]

We explore normal modes of oscillation by considering small-amplitude periodic perturbations about these equilibrium states. Two qualitatively different overlapping regimes of oscillatory motion are observed with discontinuous transitions at critical values of the central dipole strength. These critical values agree with those found by Smith et al. by considering transitions in the magnetostatic potential energy.[14] For vanishing central dipole strength, our numerical results agree with analytical calculations by Stump et al.[6] At very large values of the central dipole strength, our numerical results converge to our analytical calculations for an infinitely strong central dipole.

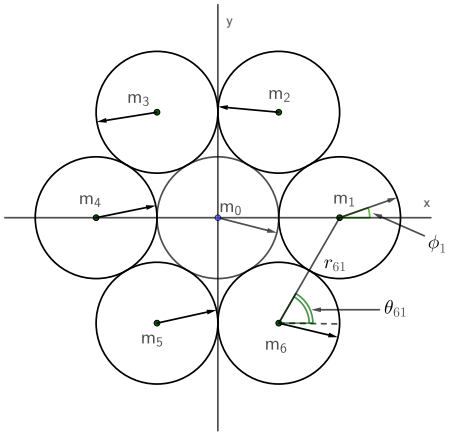

FIG. 1: Schematic diagram defining the variables used to depict six dipoles arranged at the vertices of a regular hexagon with a seventh dipole at the center. Dipole orientations are denoted by arrows, with ϕ_i denoting the angle that dipole i makes with the x-axis. The distance between dipoles i and j is denoted by r_{ij}. The angle that segment r_{ij} makes with the x-axis is denoted by θ_{ij}. The perimeter dipoles $m_1, m_2, ..., m_6$ all have the same strength m, while the central dipole may have a different strength, m_0. The presented configuration is not an equilibrium state.

II. SYSTEM AND METHODS

A. Geometry

The centers of six identical dipoles are fixed at the vertices of a hexagon, and a seventh dipole with variable strength but identical moment of inertia is fixed at the center of the hexagon. All seven are allowed to spin freely in the plane of the hexagon about axes that are perpendicular to this plane, with their magnetic moments directed parallel to this plane. The ith dipole's orientation relative to the x-axis is denoted as ϕ_i, with $i = 0, 1, 2, ..., 6$. The distance between dipoles i and j is denoted as r_{ij} and the angle of the associated line segment with the x-axis is denoted as θ_{ij} (Fig. 1).

B. Equations of Motion

We start with the magnetostatic potential energy of a pair of magnetic dipoles which are oriented in a common plane,[13]

$$U_{ij} = -U_0 \frac{C_{ij}}{2} \left(\frac{a}{r_{ij}}\right)^3 [\cos(\phi_i - \phi_j) + 3\cos(\phi_i + \phi_j - 2\theta_{ij})]. \quad (1)$$

Here,

$$U_0 = \frac{\mu_0 m^2}{4\pi a^3} \quad (2)$$

is the energy scale, μ_0 is the vacuum permeability, m is the strength of a perimeter dipole, and a is the

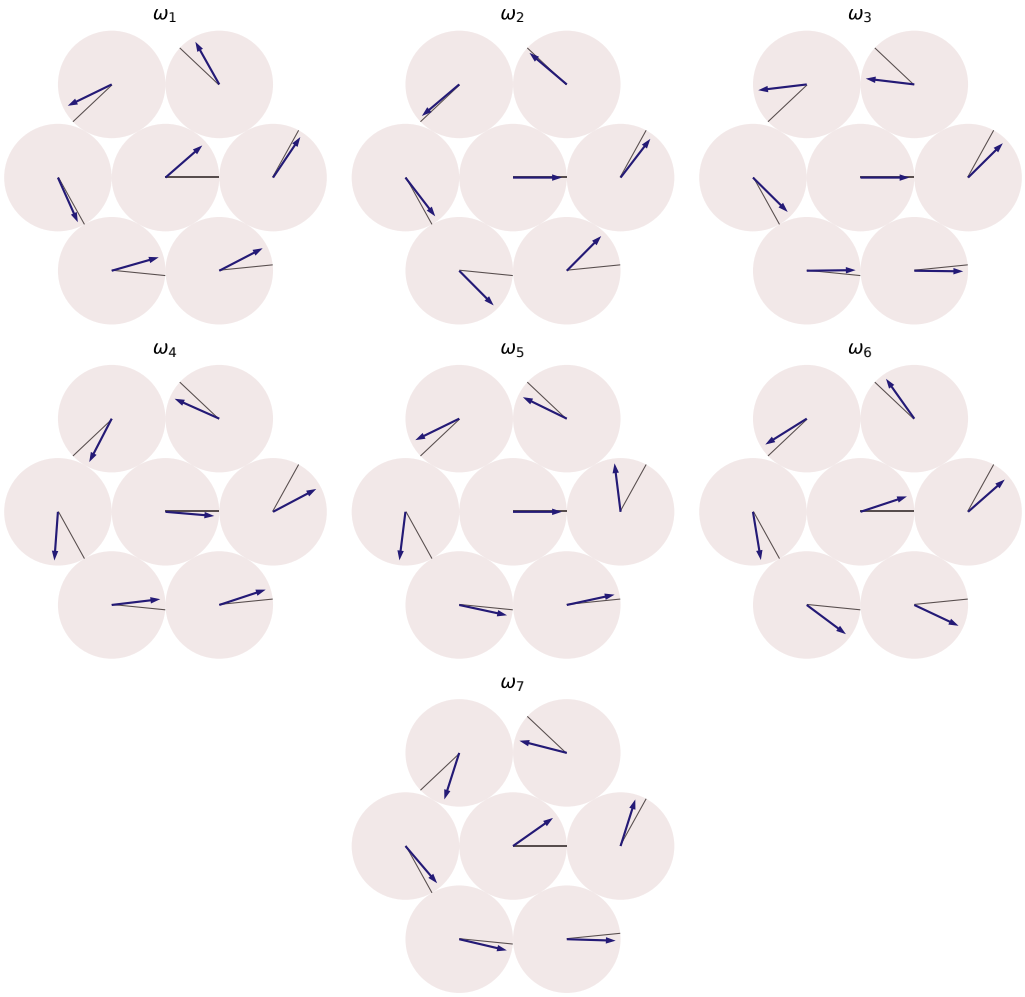

FIG. 2: Schematic representations of the seven eigenmodes of oscillation about the circular state for a central dipole with relative strength $\alpha = 1.3$. The thin lines denote the equilibrium dipole orientations for this configuration, $\vec{\phi}^*$. The arrows denote the perturbed orientations, $\vec{\phi}^* + \delta\vec{\phi}_i$.

distance between adjacent dipole centers. The coefficient

$$C_{ij} = \begin{cases} \alpha \text{ if } i = 0 \text{ or } j = 0 \\ 1 \text{ otherwise} \end{cases} \tag{3}$$

involves the ratio $\alpha = m_0/m$ of the central dipole strength m_0 to the perimeter dipole strength m. The limiting case illustrated in Fig. 1 shows $a = D$, the sphere diameter. Our calculations are also valid for $a > D$, which would apply if the dipoles were kept a fixed distance from each other by some other force. The total magnetostatic potential energy of the system is given by

$$U(\vec{\phi}) = \frac{1}{2}\Sigma_{i,j=0,i\neq j}^{6} U_{ij}, \tag{4}$$

where the factor $1/2$ ensures that each pairwise interaction is counted only once. The total kinetic en-

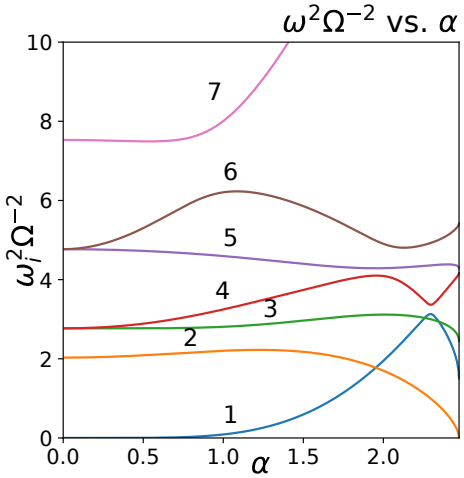

FIG. 3: Scaled frequencies ω_i of normal-mode oscillations about the circular state vs. the central dipole strength α, where Ω is the characteristic frequency.

ergy is

$$T = \frac{I}{2}\Sigma_i \dot{\phi}_i^2, \tag{5}$$

where I is the moment of inertia of a dipole. The Lagrangian and equations of motion are

$$L = T - U \tag{6a}$$

$$\frac{d}{dt}\left(\partial_{\dot{\phi}_i} L\right) = \partial_{\phi_i} L \tag{6b}$$

$$I\ddot{\phi}_i = -\partial_{\phi_i} U, \tag{6c}$$

where $\partial_{\phi_i} = \partial/\partial\phi_i$. To determine equilibrium states, we begin with the ground state of orientations found in Stump et al.[6] for hexagonally arranged dipoles and increase α incrementally from $\alpha = 0$. As the exact orientations for equilibrium depend on α, when the center dipole strength is increased by some $\Delta\alpha$, the previous orientations are no longer an equilibrium state. The system would then proceed to oscillate around the new, unknown equilibrium. We use an RK45 numerical integrator[15] to evolve the system in time. To damp these oscillations and settle into the new equilibrium, we slowly increase a damping factor γ to dissipate energy,

$$I\ddot{\phi}_i = -\partial_{\phi_i} U - \gamma\dot{\phi}_i. \tag{7}$$

The objective is to pass through critical damping and to reduce the sum of the squares of the accelerations until this sum is below a small threshold ε,

$$\Sigma_{i=0}^{6}\ddot{\phi}_i^2 < \varepsilon. \tag{8}$$

For most of the simulations, we use $\varepsilon = 10^{-8}$. Once this threshold is reached we consider the configuration to be an an equilibrium state, $\vec{\phi}^*(\alpha)$.

These equilibrium states agree with those obtained by minimizing the magnetostatic potential energy.[14] The total system's net dipole moment and potential energy undergo a bifurcation at a critical value $\alpha = \alpha_2 \approx 2.47$, above which the central magnet plays a dominant role. We therefore refer to this state as the "dipolar state." Consideration of the potential energy, the toroidal magnetic moment, and three dipole orientation angles indicates that the bifurcation at $\alpha = \alpha_2$ is a fold bifurcation.[16]

When lowering α through α_2, the dipolar state persists until a lower critical value $\alpha = \alpha_1 \approx 1.16$ is reached, below which the system reverts to the original state, called the "circular state" because of the significant role of the perimeter magnets. Thus, the system is bistable for $\alpha_1 < \alpha < \alpha_2$. Consideration of several state variables indicates that the bifurcation at $\alpha = \alpha_1$ is a subcritical pitchfork bifurcation.[16]

C. Small Amplitude Analysis

Given the equilibrium states, we linearize the acceleration terms $\ddot{\phi}_i$ in a manner similar to the one described in Taylor's Mechanics,[17]

$$I\ddot{\phi}_i \approx U_0\Sigma_j \left[\left(\partial_{\phi_j}\partial_{\phi_i}\frac{U}{U_0}\right)\Big|_{\vec{\phi}^*}\right]\phi_j. \tag{9}$$

Equation (9) is equivalent to a matrix operating on a vector, and allows us to rewrite the expression as

$$I\ddot{\vec{\phi}} = U_0\widehat{M}\vec{\phi}, \tag{10}$$

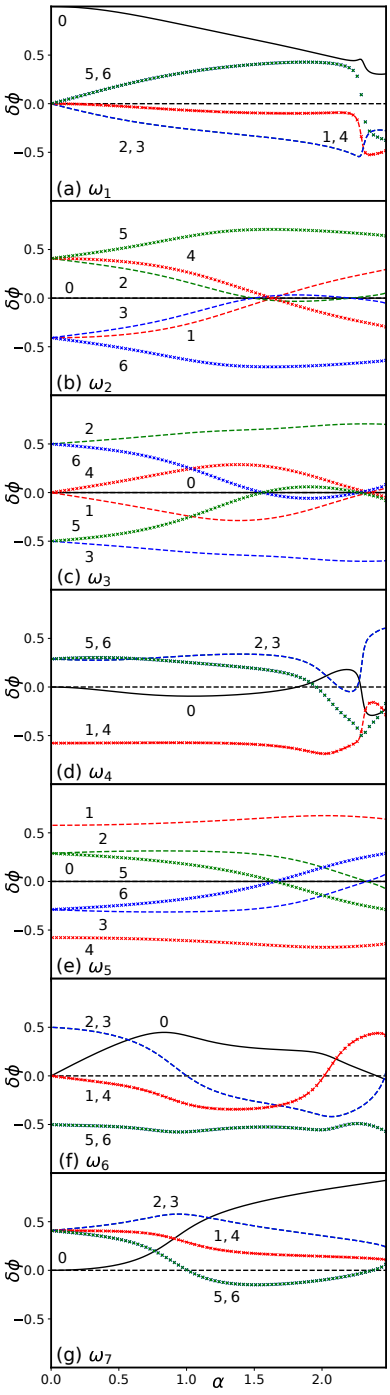

FIG. 4: Each panel depicts the normal mode of oscillation around the circular state. Dashed traces correspond to ϕ_1,ϕ_2, and ϕ_3, while the thicker markers correspond to ϕ_4, ϕ_5 and ϕ_6. The solid trace denotes the value of ϕ_0. In many cases two degrees of freedom are synchronized, in which case the variables are listed as a comma-separated pair.

where the elements of $\widehat{M}$, the Hessian matrix, are defined by

$$M_{ij} = -\left(\partial_{\phi_j}\partial_{\phi_i}\frac{U}{U_0}\right)\Big|_{\vec{\phi}^*}. \tag{11}$$

These derivatives are calculated numerically at the equilibrium orientations. We assume oscillating solutions of the form

$$\vec{\phi} = \vec{\phi}^* + \vec{\delta\phi}_i \exp(-i\omega_i t), \tag{12}$$

and reduce the problem of predicting the time evolution to an eigenvalue calculation of the form

$$\frac{-\omega_i^2}{\Omega^2}\vec{\delta\phi}_i = \widehat{M}\vec{\delta\phi}_i, \tag{13}$$

where

$$\Omega^2 = \frac{U_0}{I} \tag{14}$$

is the characteristic frequency squared.[6] Going forward we will refer to $\vec{\delta\phi}_i$ as the eigenvector for a given mode.

III. ANALYSIS

A. Comparing with Prior Results

The $\alpha = 0$ case provides an opportunity to validate our method by comparing it with the magnetic polygon analysis of Stump et al.,[6] as our $\alpha = 0$ case is equivalent to their $N = 6$ case. For N magnets located at the vertices of a regular N-gon, their normal-mode frequencies are given by

$$\omega_j^2 = \frac{\lambda_j}{I} \tag{15a}$$

$$= \Omega^2\left(Z_N + \Sigma_{\nu=1}^{N-1}\left[\frac{1+\sin^2\frac{\pi\nu}{N}}{\rho(\nu)}\right]\cos\frac{2\pi}{N}j\nu\right). \tag{15b}$$

The index j is the mode label ranging from 1 to 6 and does not map to our mode labeling because its intent is to exhaustively enumerate all the modes for

an arbitrarily sized polygon, not to name the modes in order of increasing frequency. That said,

$$\rho(n) = \frac{\sin(\pi n/N)}{\sin(\pi/N)} \tag{16}$$

is the dimensionless distance between a pair of dipoles, and

$$Z_N = \Sigma_{n=1}^{N-1} \frac{1+\cos(\pi n/N)^2}{\rho(n)^3} \tag{17}$$

is a quantity related to the potential energy per dipole.

When $N = 6$ there are four unique eigenvalues. To account for scaling factors, we compare the ratios in rising order, ω_2^2/ω_1^2 and so on. Since there are four unique eigenvalues, there will be three such ratios. To six decimals, they are 1.364407, 1.722194, and 1.578773. The values generated by our methodology agree with Stump et al. within machine precision (1 part in 10^{14}). A seventh mode exists in our system associated with the free spinning of the central magnet, as at $\alpha = 0$ the central magnet is uncoupled from the orientation of the six perimeter magnets.

B. Normal Modes of Oscillation

Figure 2 shows the normal modes of oscilllation about the circular state for $\alpha = 1.3$. Using Eq. (13) to evaluate the normal modes as a function of α, we obtain Figs. 3 and 4. These plots allow us to survey the behavior of the normal modes over the full range of the circular state.

One noteworthy feature of Fig. 3 is the splitting from four distinct modes at $\alpha = 0$, two of which are doubly-degenerate, to six distinct modes for $\alpha > 0$. Additionally, a new eigenmode (ω_1) associated with movement of the central magnet appears, and its frequency eventually surpasses the next lowest and, briefly, the third lowest.

The frequencies vary continuously throughout the process until $\alpha = \alpha_2$, where the circular state equilibrium becomes unstable through a fold bifurcation.[16] This and characteristic ratios between different coordinates that remain constant provide a consistent way to identify each mode. For example,

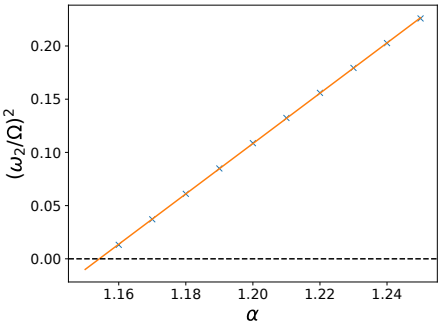

(a) Subcritical bifurcation at $\alpha_1 \approx 1.15$.

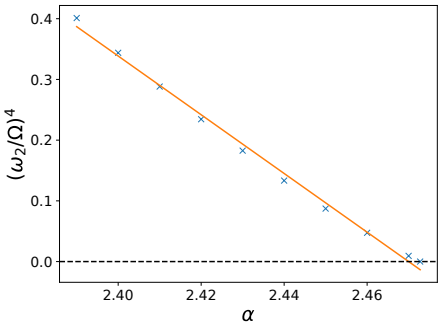

(b) Fold bifurcation at $\alpha_2 = 2.47$.

FIG. 5: Values of $(\omega_2/\Omega)^2$ from Fig. 7 near the dipolar-state subcritical bifurcation at $\alpha_1 = 1.16$ (a, data points) and values of $(\omega_2/\Omega)^4$ from Fig. 3 near the circular-state fold bifurcation at $\alpha_2 = 2.47$ (b, data points). Shown as solid traces are linear fits to the data that intersect the $\omega_2 = 0$ axis at $\alpha = \alpha_1$ (a) and $\alpha = \alpha_2$ (b).

in mode 1, $\delta\phi_1/\delta\phi_4 > 0$ so if you were calculating normal modes and unsure if a vector was associated with mode 1, 2, or 3, calculating $\delta\phi_1/\delta\phi_4$ would tell you if you had mode 1, or either mode 2 or 3.

Our frequency data support the conclusion that the instability at $\alpha = \alpha_2$ is a fold bifurcation.[16] Near such bifurcations, a normal-mode frequency vanishes according to[18]

$$\omega^2 \propto (\alpha_2 - \alpha)^{1/2}. \tag{18}$$

The linearity of $(\omega_2/\Omega)^4$ vs. α in Fig. 5b supplies evidence of this conclusion.

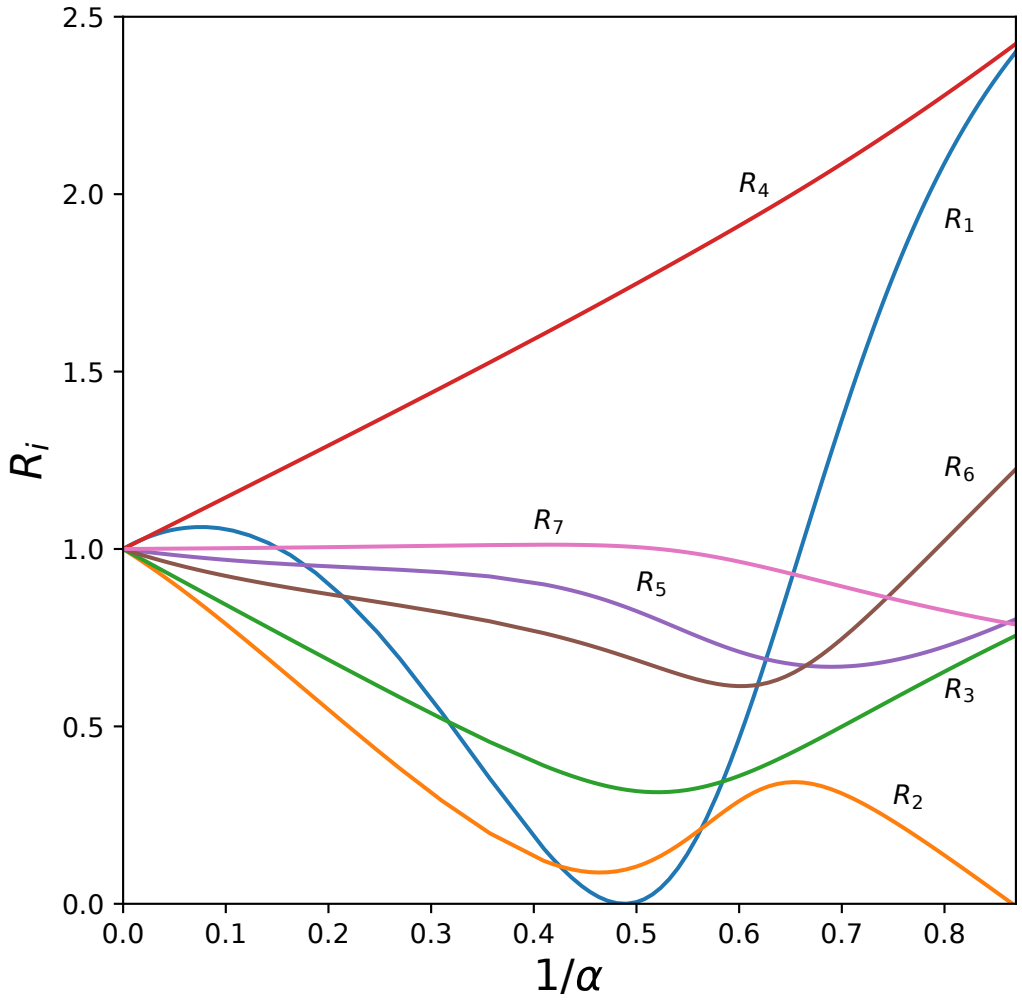

FIG. 6: R_i is the ratio of eigenvalue ω_i^2/α at α and its projected value for $\alpha \to \infty$, Ω_i. All modes of the dipolar state converge on their $\alpha \to \infty$ limiting behavior at varying rates.

C. Large α Limit

One of the difficulties in developing an analytic method for calculating the eigenmodes of this system is that the equilibria themselves are nonlinear. However, there are two values of α where the calculation is simple. Stump et al.[6] has already examined $\alpha = 0$, as was mentioned earlier, exploiting the system's strong symmetry to determine the equilibrium.

The other such case is $\alpha = \infty$. As α increases, the perimeter magnets align increasingly with the field of the central magnet. As $\alpha \to \infty$, all other interactions are overwhelmed by this field. From this we know that

$$\hat{m}_i \parallel \mathbf{B}_0 \parallel \left(2\cos^2\theta_{0i} - \sin^2\theta_{0i}\right)\hat{x} + 3\cos(\theta_{0i})\sin(\theta_{0i})\hat{y}, \tag{19}$$

where θ_{0i} is the angle defined in Sec. II A and $\mathbf{B}_0$ is the magnetic field generated by the central dipole at that location. For $i = 1,2,...,6$, these equilibrium angles are[14] 0, $\pi - \tan^{-1}(3^{3/2})$, $\tan^{-1}(3^{3/2}) - \pi$, 0, $\pi - \tan^{-1}(3^{3/2})$, $\tan^{-1}(3^{3/2}) - \pi$. Specifying these angles allows us to evaluate the elements of the linearization matrix $\widehat{M}$ in a known configuration.

It works out that $\widehat{M}$ contains terms of α to at most the first power, and is analogous to the spring constant k in a simple harmonic oscillator. As α approaches infinity, all ω_i^2 would also approach infinity. For this reason we will actually calculate the matrix $\lim_{\alpha\to\infty}(\widehat{M}/\alpha)$ which is presented here to 4 decimal places:

$$\begin{bmatrix} -9.2915 & -1.0 & -1.5118 & -1.5118 & -1.0 & -1.5118 & -1.5118 \\ -1.0 & -2.0 & 0 & 0 & 0 & 0 & 0 \\ -1.5118 & 0 & -1.3228 & 0 & 0 & 0 & 0 \\ -1.5118 & 0 & 0 & -1.3228 & 0 & 0 & 0 \\ -1.0 & 0 & 0 & 0 & -2.0 & 0 & 0 \\ -1.5118 & 0 & 0 & 0 & 0 & -1.3228 & 0 \\ -1.5118 & 0 & 0 & 0 & 0 & 0 & -1.3228 \end{bmatrix}, \tag{20}$$

for which computer algebra systems[19] can readily determine the eigenvalues. These values correspond to $-\omega_i^2/\Omega^2\alpha$ and are, to 4 decimal places, -0.1815, -1.3229, -1.9126, -2.0000, and -10.5203. The second-lowest mode is triply degenerate. We will refer to these as Ω_i^2 where

$$\lim_{\alpha\to\infty} \frac{\omega_i^2}{\Omega^2\alpha} = \Omega_i^2. \tag{21}$$

To compare Ω_i with the normal modes of the system at other values of α we define a ratio,

$$R_i = \frac{\omega_i^2}{\alpha\Omega^2}\frac{1}{\Omega_i^2}, \tag{22}$$

that captures how well a mode's eigenvalue matches its limiting behavior, with 1 being an exact match. Figure 6 is a plot of R_i vs. $1/\alpha$.

The limiting behavior in Fig. 6 for $\alpha \to \infty$ supports the claim that the process used for intermediate values is sound. The values for the eigenvalues and corresponding modes are produced much like the circular state and are presented in Figs. 7 and 8.

One point of interest is that ω_1^2 approaches 0 at $\alpha \approx 2.05$ before rebounding and then surpassing the value of ω_2^2. The value $\alpha \approx 2.05$ ($1/\alpha \approx 0.49$) corresponds to a vanishing net perimeter dipole moment. When the system is perturbed along the direction of the eigenvector for ω_1, the perimeter dipoles move in such a way that the central dipole continues to align with the magnetic field at that point, thus no torques arise. Without any restoring force for

FIG. 7: Scaled frequencies ω_i of normal-mode oscillations about the dipolar state vs. the reciprocal of the central dipole strength α, where Ω is the characteristic frequency.

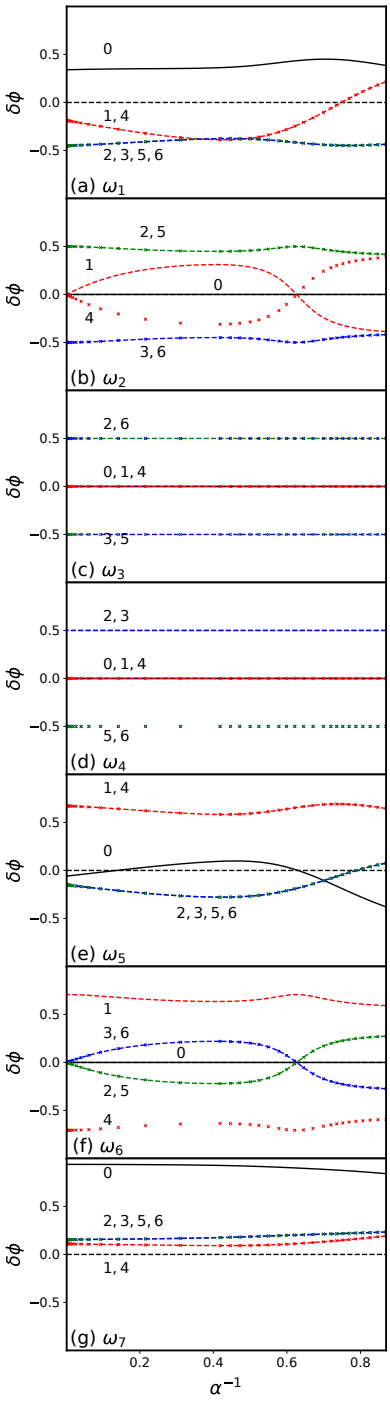

FIG. 8: Each panel depicts a normal mode of oscillation around the dipolar state. The traces are labeled in the same manner as in Fig. 4.

motion, in that direction the period is infinite. The scipy numerical processing package identifies an unstable equilibrium that has very nearly the same potential energy (a gap of approximately .011 U_0 at $\alpha \approx 2.06$), but its configuration does not match the dipolar state.

In Fig. 7, ω_2^2 drops linearly to zero as $\alpha \to \alpha_1$ from above, and becomes negative for $\alpha < \alpha_1$ (beyond the frame of Fig. 7). These data support the conclusion that the transition at $\alpha = \alpha_1$ is a subcritical pitchfork bifurcation.[16] Near such a bifurcation, a normal-mode frequency vanishes according to[18]

$$\omega^2 \propto \alpha - \alpha_1. \tag{23}$$

The linearity of $(\omega_2/\Omega)^2$ vs. α in Fig. 5a supplies evidence of this conclusion.

IV. CONCLUSIONS

A system of seven magnets presents an opportunity to examine nonlinear bifurcations and bistability in a manner that is physically realizable and has few degrees of freedom. We find that the circular and dipolar equilibrium states have qualitatively different normal modes of oscillation. Additional avenues for investigation include: What is the simplest configuration of dipoles that can exhibit nonlinear bifurcations and instability? How does a system of N magnets arranged in a circle around a central magnet behave for large N? Insights into the behavior of such large collections of dipoles may apply to models of cylindrical wave guides made of materials with significant molecular dipole moments.

V. ACKNOWLEDGEMENTS

The data that support these conclusions are available from the corresponding author upon request. We gratefully acknowledge support from NSF Grant No. 1808225.

[1] S. Borgers, S. Völkel, W. Schöpf, and I. Rehberg, "Exploring cogging free magnetic gears," *American Journal of Physics*, vol. 86, no. 6, pp. 460–469, 2018.

[2] S. Modaresahmadi, A. Hosseinpour, and W. B. Williams, "Fatigue life prediction of a coaxial multi-stage magnetic gear," in

2019 IEEE Texas Power and Energy Conference, TPEC 2019, 2019.

[3] J. Schönke, "Smooth teeth: Why multipoles are perfect gears," *Phys. Rev. Applied*, vol. 4, p. 064007, Dec 2015.

[4] O. Lourie, D. M. Cox, and H. D. Wagner, "Buckling and collapse of embedded carbon nanotubes," *Phys. Rev. Lett.*, vol. 81, pp. 1638–1641, Aug 1998.

[5] G. L. Pollack and D. R. Stump, "Two magnets oscillating in each other's fields," *Canadian Journal of Physics*, vol. 75, no. 5, pp. 313–324, 1997.

[6] D. R. Stump, G. L. Pollack, and J. Borysowicz, "Magnets at the corners of polygons," *American Journal of Physics*, vol. 65, no. 9, pp. 892–897, 1997.

[7] S. Kantorovich, A. O. Ivanov, L. Rovigatti, J. M. Tavares, and F. Sciortino, "Nonmonotonic magnetic susceptibility of dipolar hard-spheres at low temperature and density," *Phys. Rev. Lett.*, vol. 110, p. 148306, Apr 2013.

[8] B. F. Edwards, D. M. Riffe, J. . Ji, and W. A. Booth, "Interactions between uniformly magnetized spheres," *American Journal of Physics*, vol. 85, no. 2, pp. 130–134, 2017.

[9] S. Hartung, F. Sommer, S. Völkel, J. Schönke, and I. Rehberg, "Assembly of eight spherical magnets into a dotriacontapole configuration," *Physical Review B*, vol. 98, no. 21, p. 214424, 2018.

[10] B. F. Edwards and J. M. Edwards, "Periodic nonlinear sliding modes for two uniformly magnetized spheres," *Chaos*, vol. 27, no. 5, 2017.

[11] B. F. Edwards, B. A. Johnson, and J. M. Edwards, "Periodic bouncing modes for two uniformly magnetized spheres. i. trajectories," *Chaos: An Interdisciplinary Journal of Nonlinear Science*, vol. 30, no. 1, p. 013146, 2020.

[12] B. F. Edwards, B. A. Johnson, and J. M. Edwards, "Periodic bouncing modes for two uniformly magnetized spheres. ii. scaling," *Chaos: An Interdisciplinary Journal of Nonlinear Science*, vol. 30, no. 1, p. 013131, 2020.

[13] P. T. Haugen and B. F. Edwards, "Dynamics of two freely rotating dipoles," *American Journal of Physics*, vol. 88, no. 5, pp. 365–370, 2020.

[14] A. D. P. Smith, P. T. Haugen, and B. F. Edwards, "Hysteretic transition between states of a filled hexagonal magnetic dipole cluster," *Journal of Magnetism and Magnetic Materials*, vol. 549, p. 168991, 2022.

[15] E. Fehlberg, *Low-order Classical Runge-Kutta Formulas with Stepsize Control and Their Application to Some Heat Transfer Problems*. NASA technical report, National Aeronautics and Space Administration, 1969.

[16] S. Völkel, S. Hartung, and I. Rehberg, "Comment on 'Hysteretic transition between states of a filled hexagonal magnetic dipole cluster'," *Journal of Magnetism and Magnetic Materials, in press*, 2022.

[17] J. R. Taylor, *Classical Mechanics*. University Science Books, 2005.

[18] S. Strogatz, *Nonlinear Dynamics and Chaos: With Applications to Physics, Biology, Chemistry, and Engineering*. CRC Press, 2018.

[19] C. R. Harris, K. J. Millman, S. J. van der Walt, R. Gommers, P. Virtanen, D. Cournapeau, E. Wieser, J. Taylor, S. Berg, N. J. Smith, R. Kern, M. Picus, S. Hoyer, M. H. van Kerkwijk, M. Brett, A. Haldane, J. F. del R'ıo, M. Wiebe, P. Peterson, P. G'erard-Marchant, K. Sheppard, T. Reddy, W. Weckesser, H. Abbasi, C. Gohlke, and T. E. Oliphant, "Array programming with NumPy," *Nature*, vol. 585, pp. 357–362, Sept. 2020.